Arabinogalactan prevented APAP-induced acute liver injury by regulating the intestinal flora in mice

Dongxu Wang
Jilin Agricultural Science and Technology University
Shengxue Zhou (zhoushengxue1111@163.com)
Jilin Agricultural Science and Technology University
Xiuying Wang
Jilin Agricultural Science and Technology University

Article

Keywords: AG, APAP, intestinal flora, liver-gut interaction, PI3K, AKT, NF-κB, liver injury, Apoptosis

Posted Date: April 6th, 2022

DOI: https://doi.org/10.21203/rs.3.rs-1380093/v2

Abstract

Background: This study aimed to explore the mechanism by which arabinogalactan (AG) inhibited N-acetyl-para-aminophenol (APAP)-induced acute liver injury in mice. The balance of the mouse intestinal flora and the relationship between AG treatment and the PI3K/AKT and NF-κB signaling pathways were evaluated to confirm a liver-gut interaction. Methods: Mice were administered 2 different doses of AG (150 or 300 mg/kg body weight) by gavage for 7 days and liver injury was induced by a single injection of APAP (250 m/kg). Hematoxylin-eosin staining, terminal deoxynucleotidyl transferase dUTP nick-end labeling, and Hoechst 33258 fluorescence staining of liver tissue were used to analyze liver damage. Western blots were used to evaluate expression of proteins related to PI3K/AKT and NF-κB signaling pathways, and changes in the hierarchical structure of the intestinal flora were determined. Results: AG pretreatment increased the proportion of Lactobacillus and decreased the abundance of species from norank_o_Clostridiaceae and Prevotella in mouse feces compared with APAP-only treated mice. AG pretreatment reversed glutathione depletion and CYP2E1 overexpression, reduced the production of malondialdehyde and 4-hydroxynonenal, and decreased the levels of alanine aminotransferase, aspartate aminotransferase, tumor necrosis factor-α and interleukin-1β compared with the APAP-only treated mice. The levels of proteins related to the PI3K/AKT signaling pathway were similar between the AG and control groups. AG pretreatment significantly reduced APAP-induced hepatocyte apoptosis and necrosis and inflammatory infiltration into the liver. Conclusion: PI3K/AKT pathway-mediated BAX expression and the NF-κB signaling cascade were inhibited by AG. AG protected the intestinal flora composition, which subsequently suppressed oxidative stress in the liver, improved the inflammatory response, and reduced hepatocyte apoptosis and necrosis.

Background

The liver is the largest organ in the human body and participates in nutrient and drug metabolism and detoxification of xenobiotics. Through the continuous in-depth study of the “intestine-liver” axis [1], it has been demonstrated that the occurrence and development of liver disease is closely related to changes in the intestinal flora. Recent studies have found that the role of intestinal flora in liver diseases is mainly mediated through inflammatory signaling pathways that are triggered by the interaction between intestinal bacteria, the liver, and the immune system [2–3]. Liver disease can cause portal hypertension and change the structure of the intestinal wall by inducing vascular congestion, edema, fibrous hyperplastic layering, thickening of the mucosal layer, and reduction or loosening of tight junctions. These changes result in increased intestinal permeability and species imbalance within the intestinal flora, thereby destroying the integrity of the intestinal barrier and causing the “intestinal leakage” phenomenon [4], which leads to bacterial translocation. The metabolites of the intestinal flora enter the liver through the intestinal hepatic circulation and activate liver-related immune cells, which may release inflammatory factors and trigger a series of inflammatory reactions, including the release of interleukin (IL)-1β from Kupffer cells. In addition, bacterial metabolites also induce monocytes to release tumor necrosis factor (TNF)-α, which acts on intestinal epithelial cells and increases intestinal permeability [5].

Subsequently, the intestinal barrier is further destroyed, which aggravates bacterial translocation, and the disease worsens leading to further complications.

Excessive use of N-acetyl-para-aminophenol (APAP), also known as acetaminophen, can cause acute liver injury [6,7]. Approximately 5–9% of APAP is metabolized by cytochrome P450 (CYP) enzymes [8] and is converted mainly into the highly reactive intermediate metabolite N-acetyl-p-benzo-quinone imine (NAPQI) by CYP2E1 [9,10]. Normally, NAPQI is rapidly detoxified by binding to glutathione (GSH). However, when APAP is excessive, the corresponding increase in NAPQI levels will consume existing GSH, and the remaining NAPQI will react with cell membrane molecules, especially by covalently binding to sulfhydryl groups in mitochondrial proteins, which may lead to mitochondria oxidative stress and dysfunction. Excess NAPQI may further trigger a massive release of endotoxin, IL-1β, TNF-α, and other inflammatory factors [11], resulting in increased intestinal permeability, an imbalance of intestinal flora, a series of liver-gut axis reactions, and related liver complications.

Arabinogalactan (AG) is a long, highly branched neutral polysaccharide composed of arabinose and galactose [12]. The main chain of AG is galactan, and its branches are predominantly arabinose side chains, which are connected to galactose through β-1,3 or β-1,6 bonds [12]. AG is a water-soluble polysaccharide. Studies have shown that AG can regulate human intestinal flora [13–14], enhance the abundance of beneficial flora, and subsequently modulate human metabolism. In this study, we focused on the regulation of intestinal flora by AG [15] to delineate molecular mechanisms by which APAP induces liver toxicity *in vivo* and evaluate the mechanistic activity of AG in liver protection. Therefore, this study aimed to evaluate the role of AG as a hepatoprotective candidate for reducing liver damage after APAP treatment.

Methods

Chemical compounds and reagents

AG (No. ECLA-JASTC-210308) with a 90% purity was purchased from Changchun Zhongxinhengyuan Co. (Changchun, China). APAP was purchased from Yansheng Biotech Co., Ltd. (Shanghai, China). The rabbit monoclonal anti-mouse AKT, phospho (p)-AKT, BAX, BCL-2, CYP2E1, 4-HNE, GAPDH, IKKα, IKKβ, p-IKKα/β, I-κBα, p-I-κBα, PI3K, p-PI3K, NF-κB p65, and p-NF-κB p65 antibodies were obtained from Cell Signaling Technology (Danvers, MA, USA). TNF-α and IL-1β ELISA kits were purchased from R&D Systems (Minneapolis, MN, USA). Hematoxylin and eosin (HE) dyes, and alanine aminotransferase (ALT), aspartate aminotransferase (AST), malondialdehyde (MDA), and GSH assay kits were purchased from Nanjing Jiancheng Institute of Biotechnology (Nanjing, China). The Hoechst 33258 dye kit was purchased from Beyotime Biotechnology Co., Ltd. (Shanghai, China). Terminal deoxynucleotidyl transferase dUTP nick-end labeling (TUNEL) apoptosis detection kits were obtained from Roche Applied Science (Shanghai, China). The DyLight 488-SABC immunofluorescence staining kit was purchased from Boster Biological Technology Co., Ltd. (Wuhan China). The remaining reagents were analytical grade and provided by Beijing Chemical Works (Beijing, China).

Animals and treatment

Male ICR mice weighing 20–25 g (Certificate No. JLUN [JI] 2021 − 0302) were purchased from JILIN University (Changchun, China). All mice that each mouse was housed in a separate cage were housed in plastic-bottomed cages with reticulate stainless-steel covers under controlled light conditions (12-h light-dark cycle). All animal protocols were conducted strictly in accordance with the Regulation on Management of Experimental Animals issued by the Ethical Committee for Laboratory Animals at Jilin Agricultural Science and Technology College (Permit No. ECLA-JASTC-18065).

After a one-week acclimatization period, mice were randomly assigned to 4 groups (n = 6/group): (1) Normal control group treated with sodium carboxymethylcellulose, (2) APAP-only treated group (250 mg/kg), (3) APAP/low dose AG-treated group (250/150 mg/kg), (4) APAP/high dose AG-treated group (250/300 mg/kg). Mice from groups 3 and 4 were administered AG (150 and 300 mg/kg per day, respectively) by gavage each day for 7 days. On the seventh day, mice from groups 2, 3, and 4 were injected with a single intraperitoneal dose of APAP (250 mg/kg) 1 h after the last pretreatment with AG. The experiment ended 24 h after APAP injections. Fecal samples were collected from all mice, immediately transferred to pre-labeled centrifuge tubes, and frozen in liquid nitrogen until further processing. All mice were euthanized by cervical dislocation, and blood was collected and centrifuged at 3000 × g for 10 min. Serum was collected and stored at − 80°C until analysis. Liver tissues were collected and weighed to calculate liver indices. A portion of each liver was fixed in 10% formalin solution (m/v) for at least 24 h and embedded in paraffin for tissue sectioning. The remaining liver tissue was rapidly frozen in liquid nitrogen and stored at − 80°C for subsequent preparation of tissue homogenates.

Biochemical marker assays

The liver tissues from the mice were re-suspended in PBS and centrifuged at 3000 × g for 10 min at room temperature depending on the kit protocol. The supernatants were collected for subsequent experiments, and AST, ALT, GSH, and MDA were quantified using commercially available kits. Serum samples were obtained as described above, and the concentrations of endotoxin, TNF-α, and IL-1β in sera were determined using ELISA assay kits in accordance with the manufacturers' protocols.

HE, TUNEL, Hoechst 33258, CYP2E1, and 4-HNE staining

The liver tissues were immersed in 10% formaldehyde for greater than 24 h, embedded in paraffin, and sectioned using a Leica RM2125 RTS microtome (Wetzlar, Germany). The 5 μm-thick sections were stained using HE and Hoechst 33258 dyes and the TUNEL assay in accordance with the manufacturers' protocols to verify changes in the liver tissues, including hepatocyte necrosis, apoptosis, and central hepatic vein congestion. The presence of 4-HNE and CYP2E1 in liver tissues from the different groups was detected by immunofluorescence staining with anti-4-HNE (1: 200) and anti-CYP2E1 (1: 200) antibodies as previously described with minor modifications [19, 20]. The degree of liver apoptosis was evaluated by quantifying the fragmented and condensed staining patterns using Image-Pro Plus 6.0 software (Media Cybernetics; Rockville, MD, USA) .

Western blot analysis

Liver tissues (200 mg) were homogenized in 2 mL RIPA buffer, and protein concentrations were determined with the BCA protein assay kit. Samples were denatured at 100°C for 5 min and stored at − 80°C until analysis by western blotting. Equal amounts of protein (20 μg/lane) were resolved by 10% sodium dodecyl sulfate-polyacrylamide gel electrophoresis and transferred to nitrocellulose membranes. The following primary antibodies were used to hybridize with the nitrocellulose membranes: antibodies against AKT, p-AKT, BAX, BCL-2, CYP2E1, 4-HNE, GAPDH, IKKα, IKKβ, p-IKKα/β, I-κBα, p-I-κBα, PI3K, p-PI3K, NF-κB p65, p-NF-κB and p65. The protein signals were quantified using densitometric analysis (GS-900, Bio-Rad Laboratories, Hercules, CA, USA).

Analysis of the composition of the mouse intestinal flora

Twenty-four h after the intraperitoneal injection of APAP, the feces from each group of mice were collected, placed in a 10 mL dry sterilized centrifuge tube, and stored at − 80°C prior to testing. The QIAamp DNA Stool Mini Kit (QIAGEN; Hilden, Germany) was used to extract bacterial genomic DNA, and all operations were performed in strict accordance with the requirements of the kit. The extracted genomic DNA was stored at − 20°C after concentration and purity determinations. The fecal flora composition was analyzed by automated ribosomal intergenic-spacer analysis, and the PCR amplification primers were: ITS-F, 5 -GTCGTAACAAGGTAGCCGTA-3 ; ITS-R, 5 - GCCAAGGCATCCAC-3 . Five μL of PCR amplification product was removed for community composition analysis using an ABI PRISM 3100 Genetic Analyzer (Thermo Fisher Scientific, Waltham, MA, USA). The sequencing data was compared through the HENUO bioinformation i-singer cloud platform. The species abundance for each sample was quantified at different classification levels, and the composition of the intestinal bacterial community was analyzed.

Statistical analysis

All data are presented as means ± SD. Statistical analyses were performed using SPSS 17.0 (SPSS Inc., Chicago, IL, USA), and significance was verified via one-way ANOVA. The p values < 0.05 were considered statistically significant.

Results

AG-induced changes in gut microbiota composition

The results based on hierarchical cluster showed that the intestinal flora compositions from each AG treatment group were clearly aggregated, while the APAP-only group was separated from the other three groups (Fig. 1A). As expected, AG treatment maintained the similarity with the overall intestinal flora composition of the control group, indicating that AG had a substantial effect on the composition of the intestinal flora after APAP-induced liver injury. Figure 1A demonstrates that the greatest distance was observed between both the control and high-dose AG (300 mg/mL) groups and the APAP-only treated group. The distribution of the low-dose AG (150 mg/mL) group was relatively scattered between the high-

dose AG group and the APAP-only group. These data indicated that the species composition of the intestinal flora of the high-dose AG group was similar to that of the control group.

Taxonomic analysis showed five main phyla in the fecal microbiota, which were Firmicutes, Bacteroidetes, Proteobacteria, Actinobacteria, and Tenericutes(Fig. 1B). In each group, the relative abundance of the phyla Firmicutes and Bacteroidetes was higher than the other phyla, and the abundance of the phylum Firmicutes was significantly higher than that of Bacteroidetes (Fig. 1B). Compared with that of the control group of mice, the proportion of Firmicutes bacteria in the feces was significantly reduced in the APAP-only treated group, and the proportion of Bacteroidetes bacteria was significantly increased. The relative abundance of Firmicutes bacteria in the feces of the two AG treatment groups was significantly higher than that of the APAP-only group, while the abundance of Bacteroidetes bacteria decreased. Furthermore, the abundance of each phylum in the high-dose AG group was similar to that of the control group (Fig. 1B and C).

The family classifications of the intestinal flora from each mouse group consisted mainly of *Lactobacillaceae*, *Muribaculaceae* (also known as S24-7), *Ruminococcaceae*, norank_o_*Clostridiaceae*, *Lachnospiraceae*, and *Prevotellaceae* (Fig. 2A). Compared with that of the bacteria in the control group, the relative abundance of *Lactobacillaceae* bacteria in the APAP-only treated group was significantly reduced, and the abundance of *Ruminococcaceae*, norank_o_*Clostridiaceae*, *Lachnospiraceae*, and *Prevotellaceae* was significantly increased. Compared with the APAP-only treatment group, both AG treatment groups had a significant increase in the abundance of *Lactobacillaceae* bacteria. The abundance of norank_o_*Clostridiaceae* in the high-dose AG group was similar to that of the control group, while the relative abundance of this family of bacteria in the low-dose AG group was similar to the APAP-only treatment group. The proportion of *Prevotellaceae* bacteria in the intestines of mice from each AG treatment group was significantly reduced compared to APAP-only treatment grou.(Fig. 2B).

At the genus level (Fig. 2C, the intestinal flora of each group of mice was predominantly composed of *Lactobacillus*, norank_f_S24_7, norank_o_*Clostridium*, *Ruminococcus*, norank_f_*Ruminococcus*, norank_f_*Lachnospira*, *Oscillospira*, and *Prevotella*. The abundance of intestinal lactobacilli in the APAP-only treatment group was reduced, and the relative abundance of norank_o_*Clostridium*, norank_f_*Ruminococcus*, *Oscillospira*, and *Prevotella* increased significantly compared with that in the control group. However, the proportion of lactobacilli in the intestines of mice in both the high- and low-dose AG treatment groups was increased significantly, while the relative proportions of norank_o_*Clostridium* and *Prevotella* were decreased compared with the APAP-only treated group (Fig. 2D).

Effects of AG on inflammatory factors and endotoxins in mice with liver injury caused by APAP

The levels of endotoxin and inflammatory factors in the sera were measured to determine the effects of AG on the intestinal flora and liver and evaluate intestinal permeability. The blood endotoxin level was significantly higher in the APAP-only treatment group than that in the control and AG groups. The control and high-dose AG treatment groups demonstrated similar endotoxin levels (Fig. 3A). Similarly, the serum

levels of TNF-α (Fig. 3B) and IL-1β (Fig. 3C) in the APAP-only group were higher than those in the control group. The serum levels of TNF-α and IL-1β in the AG-treated groups showed a downward trend, and the cytokine levels in the high-dose AG group were similar to those in the control group ($p < 0.05$ or $p < 0.01$). These results suggest that the permeability of the mouse intestine may be adjusted through the effects of AG on the intestinal flora in mice treated with APAP, which may in turn protect the intestines, liver, and other organs.

NF-κB regulates the transcription of several pro-inflammatory cytokines [3,16]. Therefore, the expression of phosphorylated and non-phosphorylated forms of proteins in the NF-κB signaling pathway were analyzed in liver tissues using western blots (Fig. 3D, E) to evaluate signaling molecules that may be related to liver protection. APAP induced a general increase in the expression levels of p-IKKα/β, p-NF-κB and p-IκBα in liver tissues; however, expression of these proteins was reduced after both high- and low-dose AG pretreatment. These data indicated that AG inhibited activation of the NF-κB signaling pathway and significantly down-regulated the expression levels of NF-κB-related proteins ($p < 0.05$ or $p < 0.01$).

The effect of AG on the liver index of mice

The weights of the mice in the control group increased, and they remained healthy. Compared with body weights for the control and AG treatment groups, after the seventh day of AG administration, the weights of the mice in the APAP-only treatment group were significantly decreased. The body weights of the mice in the high-dose group were similar to that in the control group. The indices for liver from the APAP-only group were greater than that of the control and AG groups ($p < 0.01$). The data for the AG groups were similar to that of the control group, which indicated that AG had a positive effect on mouse livers and spleens.

The effects of AG on mouse hepatocyte necrosis

As shown in Fig. 4A, hepatic cavitation was observed during the microscopic evaluation of APAP-injured mouse livers, and this phenomenon was not found in the liver tissues of control mice, which displayed normal hepatocyte structures. Evaluation of liver tissue from the low-dose AG group revealed some hepatic cavitation; however, no cavitation was observed in the high-dose AG group. These results support the conclusion that AG pretreatment reduced liver damage induced by APAP, and the protective effect was dose-dependent ($p < 0.01$ or $p < 0.05$).

The effect of AG on mouse hepatocyte apoptosis

According to Hoechset 33258 staining of nuclei (Fig. 5A) and data analysis (Fig. 5B), greater than 60% of hepatocytes from APAP-only treated mice were apoptotic, while apoptosis was decreased in the AG pretreatment groups. Apoptosis in the high-dose AG group (300 mg/kg) was reduced to approximately 30%, which was similar to the control group (24%) ($p < 0.01$). To further verify that AG treatment prevented liver injury, the TUNEL assay was used to investigate hepatocyte apoptosis. As shown in Fig. 6A and B, hepatocyte apoptosis in the APAP-only treated was greater than 80%, a result similar to Hoechset 33258

staining, while AG pretreatment substantially reduced apoptosis. The rate of apoptosis in hepatocytes from the high-dose AG treatment group (300 mg/kg) was 19%, which was similar to that of the control group (15%).

To explore the mechanism by which AG pretreatment inhibited hepatocyte apoptosis, western blots were used to detect the expression levels of apoptosis-related proteins (Figs. 6C, D). In APAP-only treated mice, the expression levels of the anti-apoptotic protein BCL-2 were decreased, whereas the pro-apoptotic protein BAX was increased in liver tissue compared with those in the control group. This phenomenon was reversed in the the high-dose AG pretreatment group, which showed expression levels similar to the control group ($p < 0.05$ or $p < 0.01$). The expression of AKT and p-PI3K in the livers was also measured (Figs. 6C, D). After APAP injection, the PI3K was decreased and AKT was increased significantly in mouse livers, while AKT was reduced and p-PI3K was increased in the livers of mice pretreated with AG. However, the expression of PI3K showed an upward trend, and PI3K unphosphorylated expression in the high-dose AG treatment group was similar to that in the control group, which further verified the effect of AG on APAP-induced liver injury in mice ($p < 0.05$ or $p < 0.01$).

The effect of AG on liver tissue changes in mice

The concentrations of GSH, MDA, ALT, and AST were measured and the expression of CYP2E and 4-HNE were analyzed in the livers to explore the protective mechanisms of AG. Compared with those in the control group, the liver GSH levels in the APAP-only treated group were significantly decreased ($P < 0.05$), while the GSH levels in the AG pretreatment groups were increased (Fig. 7A). Both AG pretreatments (high- and low-dose) alleviated APAP-induced liver damage. These data indicated that AG could effectively inhibit APAP-induced damage from oxidative stress ($p < 0.01$). The concentrations of MDA also indicated that AG effectively protected the liver from APAP-induced damage. The MDA levels in the high-dose AG group were similar to that in the control group, which were significantly lower than those in the APAP-only treated group ($p < 0.01$) (Fig. 7B). ALT and AST are important indicators used to evaluate liver damage. In the APAP-only treatment group, the levels of ALT were decreased, while AST levels were increased. However, the concentrations of ALT and AST were similar to the control group in both AG pretreatment groups and were significantly different from the APAP-only group ($p < 0.01$) (Fig. 7C).

The liver tissue sections demonstrated that the degree of liver damage was more serious in the APAP-only treatment group compared with that in the control and AG pretreatment groups. Therefore, it was not difficult to conclude that AG treatment had a protective effect on liver injury. This result was further confirmed by analyzing the expression of CYP2E and 4-HNE in liver tissue sections (Fig. 7D, E). Strong fluorescent signals for CYP2E1 and 4-HNE were observed after APAP-induced liver injury. Mice pretreated with AG (150 mg/kg and 300 mg/kg) for seven days showed reduced levels of CYP2E1 and 4-HNE. The fluorescence signals in the liver tissue from the high-dose group were similar to that found in the control group, and the same situation was verified by further analysis of the data in Fig. 7D. It can be concluded that APAP-mediated liver damage could be at least partially prevented by AG through inhibition of oxidative stress.

Discussion

AG is a water-soluble polysaccharide that cannot be absorbed by the human body. In our study, its main function was to regulate the balance of intestinal flora, protect the intestinal mucosa, and then improve liver damage through intestinal repair. After injecting the mice with APAP, the intestinal flora changed significantly. Compared with those in the control group, the proportion of Firmicutes was significantly reduced, and the proportion of Bacteroides was significantly increased in the APAP-only treated group. The results of family and genera analysis showed that the relative abundance of *Lactobacillus* was significantly reduced, while the abundance of *Ruminococcus*, norank_o_*Clostridiaceae*, *Lachnospiraceae*, and *Prevotellaceae* were significantly increased. The relative abundance of Firmicutes in the AG pretreatment groups was significantly higher than that in the APAP-only group, and the abundance in the AG groups was similar to that in the control group. Similarly, the relative abundance of *Lactobacillus* increased in the AG groups and was also similar to the control group. The data suggested that AG may have inhibited the breakdown of the intestinal barrier caused by APAP. The gut microbiome plays an important role in immune function and has been implicated in several autoimmune disorders. Microbiome alterations in multiple sclerosis correlate with variations in the expression of genes involved in dendritic cell maturation, interferon signalling and NF-kB signalling pathways in circulating T cells and monocytes[17]. Intestinal flora imbalance may cause increased intestinal permeability, which may lead to increased inflammation and release of endotoxins into the blood. For this reason, the mechanism of dysbiosis leading to liver damage was further explored by measuring inflammatory factors and endotoxins.

The PI3K/AKT pathway is a classic signal transduction pathway that has been confirmed by a large number of studies. This pathway plays an important role in various physiological and pathological processes, such as cell survival and differentiation, movement, and apoptosis [18, 19]. PI3K/AKT signaling regulates the transcriptional activity of NF-κB and its downstream pathway through phosphorylation and promotion of I-κB degradation [20, 21]. The NF-κB pathway is an important signaling pathway in various diseases, including liver and inflammatory diseases. When NF-κB is activated, its downstream inflammatory proteins (TNF-α, IL-1β) are released, which can induce tissue damage and liver inflammation. In the process of liver injury, the PI3K/AKT and NF-κB pathways regulate and balance each other, and their interaction is inseparable.

The extensive use of APAP can cause liver toxicity and damage [22] and also induce intestinal flora imbalance. Imbalance in the intestinal microbiota may cause a series of inflammatory reactions and release of harmful substances, such as endotoxins, into the portal vein system, which may further induce liver damage and liver cell apoptosis. Liver damage is characterized by extensive necrosis of liver cells; rapid elevation of ALT, AST, TNF-α, and IL-1β [23]; GSH depletion; overproduction of MDA; and overexpression of CYP2E1 and 4-HNE [24]. The data obtained from AG pretreated mice showed that AG could maintain the balance of intestinal flora, protect the intestinal mucosa, regulate intestinal permeability, and decrease the levels of endotoxin and inflammatory factors. Different doses of AG suppressed APAP-induced liver GSH depletion and CYP2E1 overexpression. Furthermore, AG reduced the

production of MDA and 4-HNE; decreased the concentrations of ALT, AST, TNF-α, and IL-1β; and was effective in a dose-dependent manner. These data indicated that AG played a role in protecting the liver by regulating intestinal balance. To support the accuracy of the experimental results, HE, TUNEL, and Hoechst 33258 staining analysis were used to clearly and intuitively observe liver damage caused by APAP and the protective effect of AG pretreatment on the liver. Direct analyses of the tissues indicated that AG pretreatment protected liver cells from the damage caused by APAP.

Western blot analysis was used to evaluate the expression of PI3K and AKT and their downstream target proteins BCL-2 and BAX. The results showed that the liver damage caused by APAP was successfully inhibited by AG, and the protein level of BAX was similar to the control group after 7 days of AG pretreatment. AG pretreatment also reduced the expression of IKKα, IKKβ and I-κBα induced by APAP and successfully inhibited the activation of NF-κB. Therefore, a potential mechanism by which AG protects against APAP toxicity may involve regulating the balance of intestinal flora, which, in turn, regulates the PI3K/AKT signaling pathway and subsequently blocks NF-κB signaling.

Conclusions

The BAX and NF-κB signaling cascade mediated by the PI3K/AKT pathway was inhibited by AG. The mechanism of action may be through AG-mediated maintenance of the hierarchical structure of the intestinal flora and the ability to protect and repair the intestinal mucosa, so as to achieve selectivity and control of absorption. AG suppressed APAP-induced oxidative stress in the liver, improved the inflammatory response, and reduced hepatocyte apoptosis and necrosis. Taken together, AG treatment may be useful to reduce damage to the liver caused by excessive or long-term application of APAP drugs.

Declarations

Ethics approval and consent to participate

The experimental protocol was established, according to the ethical guidelines and was approved by theEthics Committee of Institutional Animal Care and Use Committee of Jilin Agricultural Science and Technology College.

Consent for publication

Not applicable

Availability of data and materials

All data generated or analysed during this study are included in this published article

Competing interests

The authors declare that they have no competing interests.

Funding

The study was funded by the National College Students Innovation and Entrepreneurship Training Program of China: Inflammation and apoptosis mediated by PI3K/AKT pathway to evaluate the protection of acute liver injury due to AG's regulation of intestinal flora. (No.202111439017).

AcknowledgementsAcknowledgments

We thank Susan Zunino, PhD, from Liwen Bianji (Edanz) (www.liwenbianji.cn/), for editing the English text of a draft of this manuscript. This work was supported by National College Students Innovation and Entrepreneurship Training Program: Evaluation of inflammation and apoptosis mediated by PI3K/AKT pathway Arabinogalactan modulates gut microbiota to protect against acute liver injury (Grant202111439017).

Abbreviations

AG, Arabinogalacta; ALF, acute liver failure (ALF); AKT, protein kinase B; I-κB, inhibitor kappa B; ALT, alanine aminotransferase; APAP, Acetaminophen; TNF-α, tumor necrosis factor-α; GSH, glutathione; 4-HNE, 4-hydroxynonenal; APAP, acetaminophen; PI3K, phosphatidylinositol-3-kinase; NF-κB, nuclear factor-kappa B; IKK, inhibitor kappa B kinase; AST, aspartate aminotransferase; IL-1β, interleukin-1β; MDA, malondialdehyde; CYP2E1, cytochrome P450 E

References

1. Schnabl B, Brenner D A. Interactions between the intestinal microbiome and liver diseases. Gastroenterology 2014 May;146(6):1513-24
2. Stärkel P, Schnabl B. Bidirectional communication between liver and gut during alcoholic liver disease. Semin. Liver Dis. 2016,36: 331–339.
3. Tripathi A, Debelius J, Brenner D A, Karin K, Loomba R, Schnabl B,Knight R. The gut–liver axis and the intersection with the microbiome. Nat Rev Gastroenterology & Hepatology. 2018, 15(7): 397-411
4. Yang A M, Inamine T, Katrin Hochrath K, et al. Intestinal fungi contribute to development of alcoholic liver disease. J. Clin. Invest. 2017.127: 2829–2841
5. Odenwald M A, Turner J R. The intestinal epithelial barrier: a therapeutic target? Nat. Rev. Gastroenterol. Hepatol. 2017,14: 9–21.
6. Temple AR, Lynch JM, Vena J, Auiler JF, Gelotte CK. Aminotransferase activities in healthy subjects receiving three-day dosing of 4, 6, or 8 grams per day of acetaminophen. Clin Toxicol. 2007;45:36-44.
7. Heard K, Green JL, Anderson V, Bucher-Bartelson B, Dart RC. A randomized, placebo-controlled trial to determine the course of aminotransferase elevation during prolonged acetaminophen administration. BMC Pharmacol Toxicol. 2014;15:39.

8. Zhou Y D, Hou J G, Liu W, Ren S, Wang Y P, Zhang R, Chen C, Wang Z, Li W. eng, ameliorates acetaminophen-induced hepatotoxicity by suppressing PI3K/AKT pathway-mediated inflammation and apoptosis.International immunopharmacology. 2018, 59: 21-30
9. X. Zhao, X. Cong, L. Zheng, L. Xu, L. Yin, J. Peng, Dioscin, a natural steroid saponin, shows remarkable protective effect against acetaminophen-induced liver damage in vitro and in vivo, Toxicol. Lett. 2014 (1) (2012) 69–80.
10. McGill MR, Jaeschke H. Metabolism and disposition of acetaminophen: recent advances in relation to hepatotoxicity and diagnosis. Pharm Res. 2013;30:2174-2187.
11. Xie Y, McGill MR, Du K, et al. Mitochondrial protein adducts formation and mitochondrial dysfunction during N-acetyl-m-aminophenol (AMAP)-induced hepatotoxicity in primary human hepatocytes. Toxicol Appl Pharmacol.2015;289:213-222.
12. Fincher GB, Stone BA, Clarke AE.. Arabinogalactan proteins-structure, biosynthesis, and function. Annu Rev Plant Physiol. 1983; 34:47–70.
13. Cartmell A, Munoz-Munoz J, Briggs JA, Ndeh DA, Lowe EC, Basle A, Terrapon N, Stott K, Heunis T, Gray J, Yu L, Dupree P, Fernandes PZ, Shah S, Williams SJ, Labourel A, Trost M, Henrissat B, Gilbert HJ. A surface endogalactanase in Bacteroides thetaiotaomicron confers keystone status for arabinogalactan degradation. Nat Microbiol. 2018;3:1314–1326.
14. Chen Oliver;Sudakaran Sailendharan;Blonquist Traci;Mah Eunice;Durkee Shane;Bellamine Aouatef. Effect of arabinogalactan on the gut microbiome: A randomized, double-blind, placebo-controlled, crossover trial in healthy adults. Nutrition. 2021; Apr 20;90:111273.doi: 10.1016/j.nut.2021.111273.
15. MunozMunoz Jose; Ndeh Didier; FernandezJulia Pedro; Walton Gemma; Henrissat Bernard; Gilbert Harry J. Sulfation of Arabinogalactan Proteins Confers Privileged Nutrient Status to Bacteroides plebeius. mBio. 2021; PP e0136821-e0136821
16. Shu X S, Lv J H, Tao J, et al. Antihyperglycemic effects of total flavonoids from polygonatum odoratum in STZ and alloxan-induced diabetic rats. J Ethnopharmacol, 2009, 124(3):539-543.
17. S Jangi R Gandhi LM Cox, et al. Alterations of the human gut microbiome in multiple sclerosis. Nature, Nature communacations. 2016, DOI: 10.1038/ncomms12015.
18. Zhao P, Zhao C, Li X, Gao Q, Huang L, Xiao P, Gao W. The genus polygonatum: A review of ethnopharmacology, phytochemistry and pharmacology. J. Ethnopharmacol. 2018; 214: 274-291.
19. Gu M, Zhang Y, Fan S, Ding X, Ji G, Huang C. Extracts of rhizoma polygonati odorati prevent high-fat diet-induced metabolic disorders in c57bl/6 mice. PLoS ONE. 2013;8:e81724.
20. Shu X S, Lv J H, Tao J, et al. Antihyperglycemic effects of total flavonoids from polygonatum odoratum in STZ and alloxan-induced diabetic rats. J Ethnopharmacol, 2009, 124(3):539-543.
21. Jiang Q, Lv Y, Dai W, Miao X, Zhong D. Extraction and bioactivity of polygonatum polysaccharides.Int. J. Biol. Macromol. 2013;54:131–135.
22. Chen Y, Yin L, Zhang X, Wang Y, Chen Q, Jin C, Hu Y, Wang J. Optimization of alkaline extraction and bioactivities of polysaccharides from rhizome of Polygonatum odoratum. BioMed Res. Int. 2014;2014:504896.

23. Yan H, Lu J, Wang Y, Gu W, Yang X, Yu J. Intake of total saponins and polysaccharides from polygonatum kingianum affects the gut microbiota in diabetic rats. Phytomedicine. 2017;26:45–54.
24. Wang Y, Fei Y Q, Liu L R et al. Polygonatum odoratum Polysaccharides Modulate Gut Microbiota and Mitigate Experimentally Induced Obesity in Rats. Int J Mol Sci. 2018; 19(11): 3587

Table 1

Table 1. The effect of AG on the body weight and organ index of mice with liver injury. (n=6, Mean ± SD)

Groups	Dosage	Body weight		Liver Index	Spleen Index
	(mg/mL)	Initial (g)	Final (g)	(mg/g)	(mg/g)
Normal	0	21.52±1.24	24.37±0.83	35.85±1.22	3.56±0.7
APAP	250	21.38±1.97	20.25±0.75*	40.36±1.58*	4.34±1.8**
APAP+AG	150	21.33±1.23	22.68±0.69#	36.47±0.97#	3.61±1.6##
	300	21.35±1.23	23.87±0.88#	38.67±1.14#	3.34±1.2##

(*P<0.05, **P<0.01 vs. Normal group; # P<0.05, ## P<0.01 vs. APAP group)

Figures

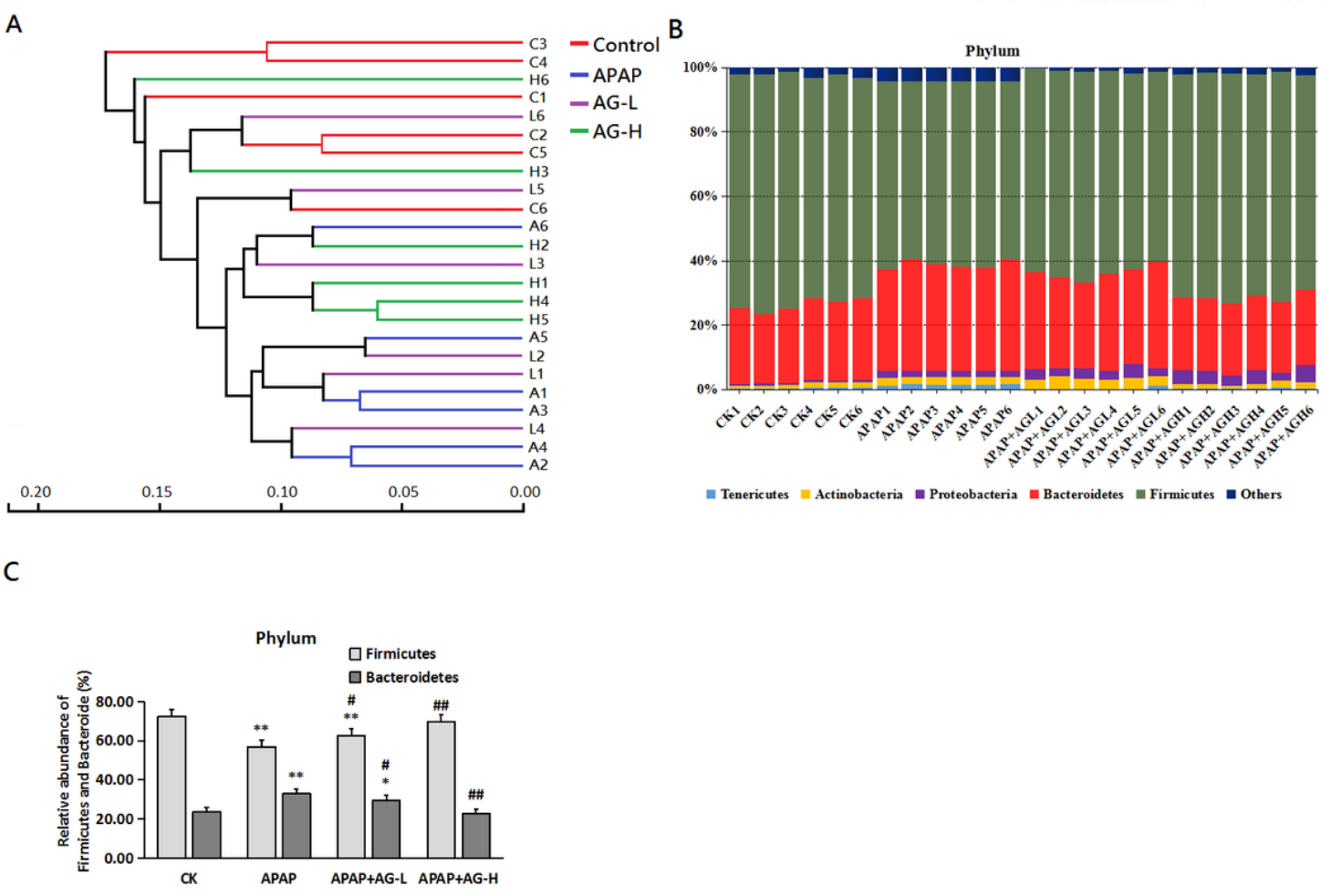

Figure 1

AG treatment regulated gut microbiota structure in APAP induced liver injury. (**A**)Hierarchical cluster analysis at the generic classification level. **(B)** Relative abundances of gut microbiota at the phylum level. (C)Firmicutes and Bacteriodetes content in Phylum level . n = 6. *p < 0.05, **p < 0.01 vs. normal control group; #p < 0.05, ##p < 0.01 vs. APAP group.

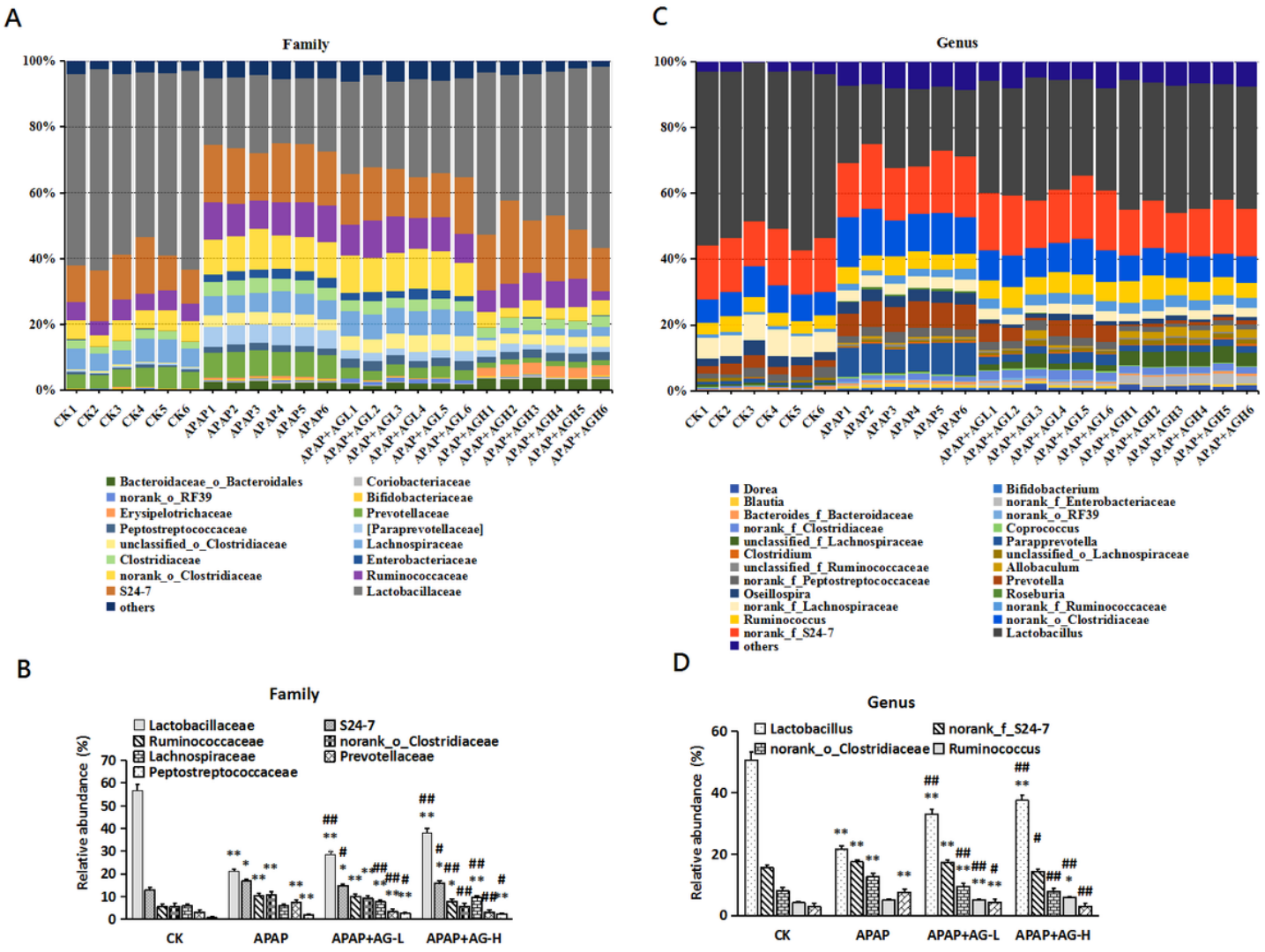

Figure 2

AG treatment regulated intestinal flora for APAP-induced liver injury. (A) Relative abundances of gut microbiota at the family leve. (B) Lactobacillus, S-24-7, Rumenococcus, nroank_o_Clostridiaceae, Lacetospirillum, and Prevotella content in Family level. (C) Relative abundances of gut microbiota at the genus level. (D) Lactobacillus, norank_f_S24_7, Rumenococcus, nroank_o_Clostridiaceae content in Genus level. n = 6. *p < 0.05, **p < 0.01 vs. normal control group; #p < 0.05, ##p < 0.01 vs. APAP group.

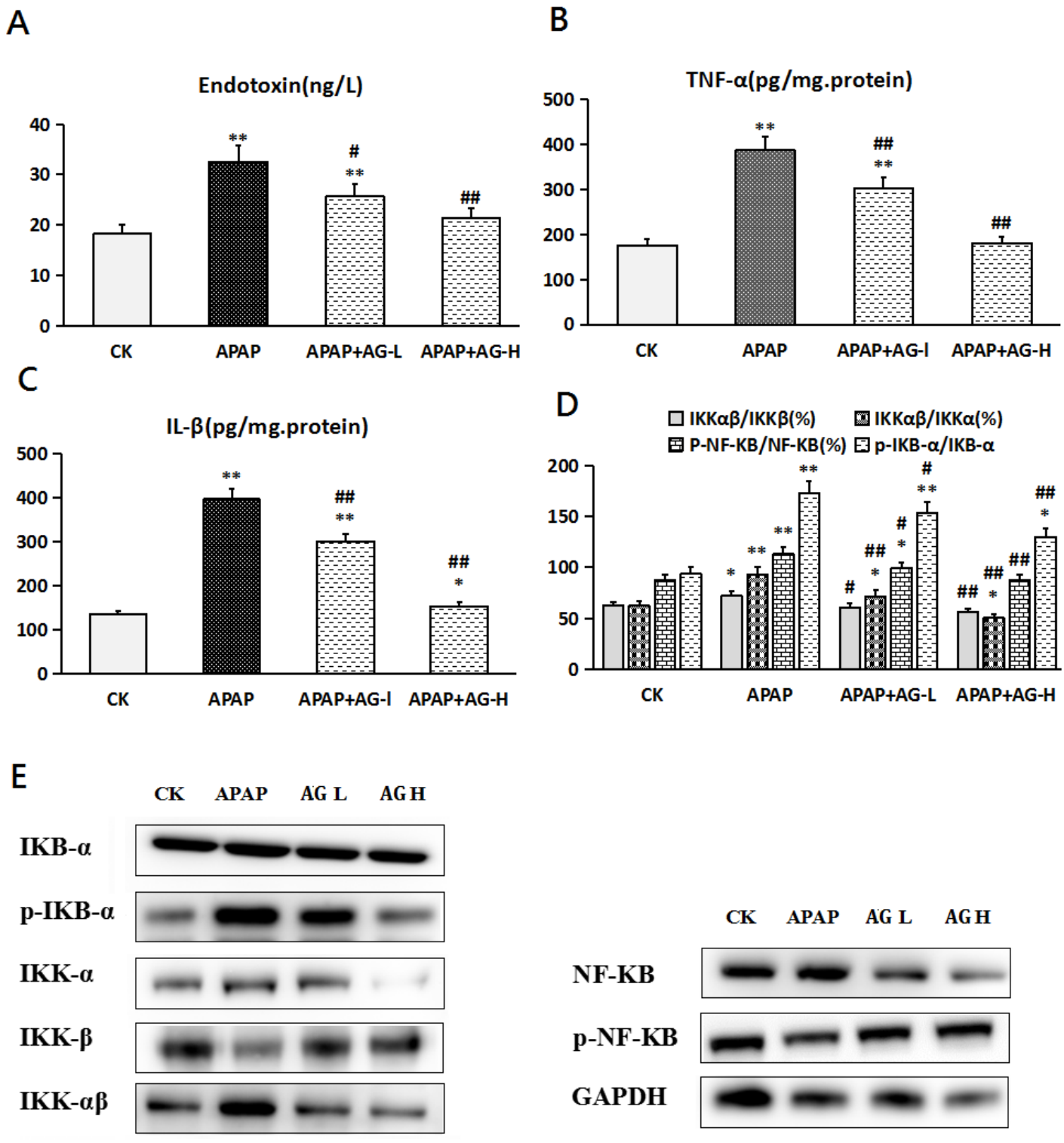

Figure 3

AG adjusts the inflammation and endotoxin content of APAP-induced liver injury in mice. (A) TNF-α level. (B) IL-1β level. (C) Endotoxin leve. Western blot analysis (D) Quantification of relative protein expression of IKKα, IKKβ, IκBα and NF-κB.(E) The protein expressions of IKB-α, p-IKB-α, IKK-α, IKK-β, p-IKKαβ, NF-KB, p-NF-KB, Values represent mean ± SE. n = 6. *p < 0.05, **p < 0.01 vs. normal control group; #p < 0.05, ##p < 0.01 vs. APAP group.

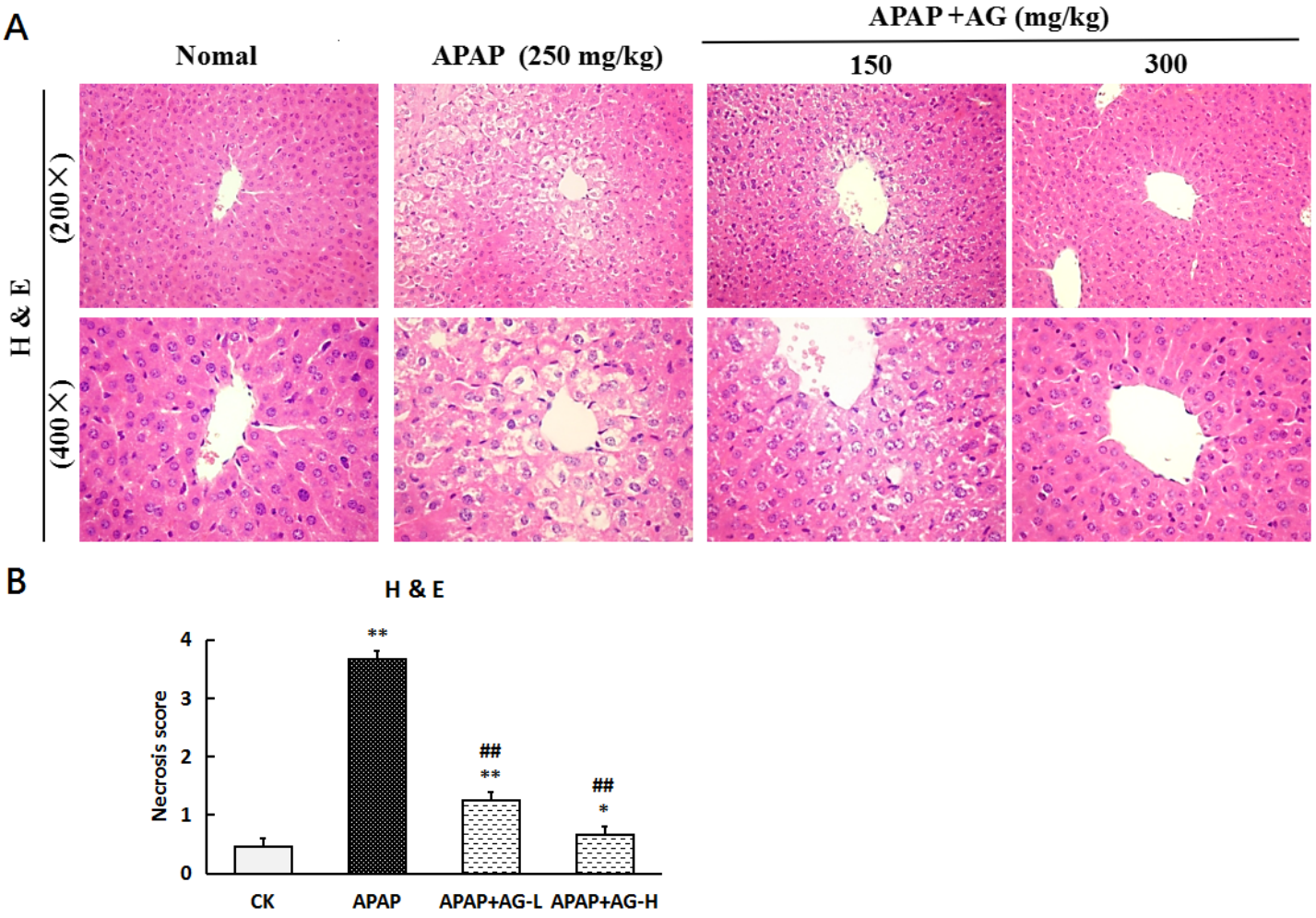

Figure 4

AG reduces necrosis in mice. **(A)** Liver tissues were stained with hematoxylin-eosin (H&E) (200×, 400×). In the H&E staining, yellow arrows indicate hepatocyte apoptosis cavitation; **(B)** Analysis of the degree of necrosis of peripheral vein cells in liver tissue. 0 = no damage, 1 = 0–10%, 2 = 11%–25%, 3 = 26%–45%, 4 = 46%–75%, 5 = > 75%. All data were expressed as mean ± S.D., n = 6. *p < 0.05, **p < 0.01 vs. normal control group; #p < 0.05, ##p < 0.01 vs. APAP group.

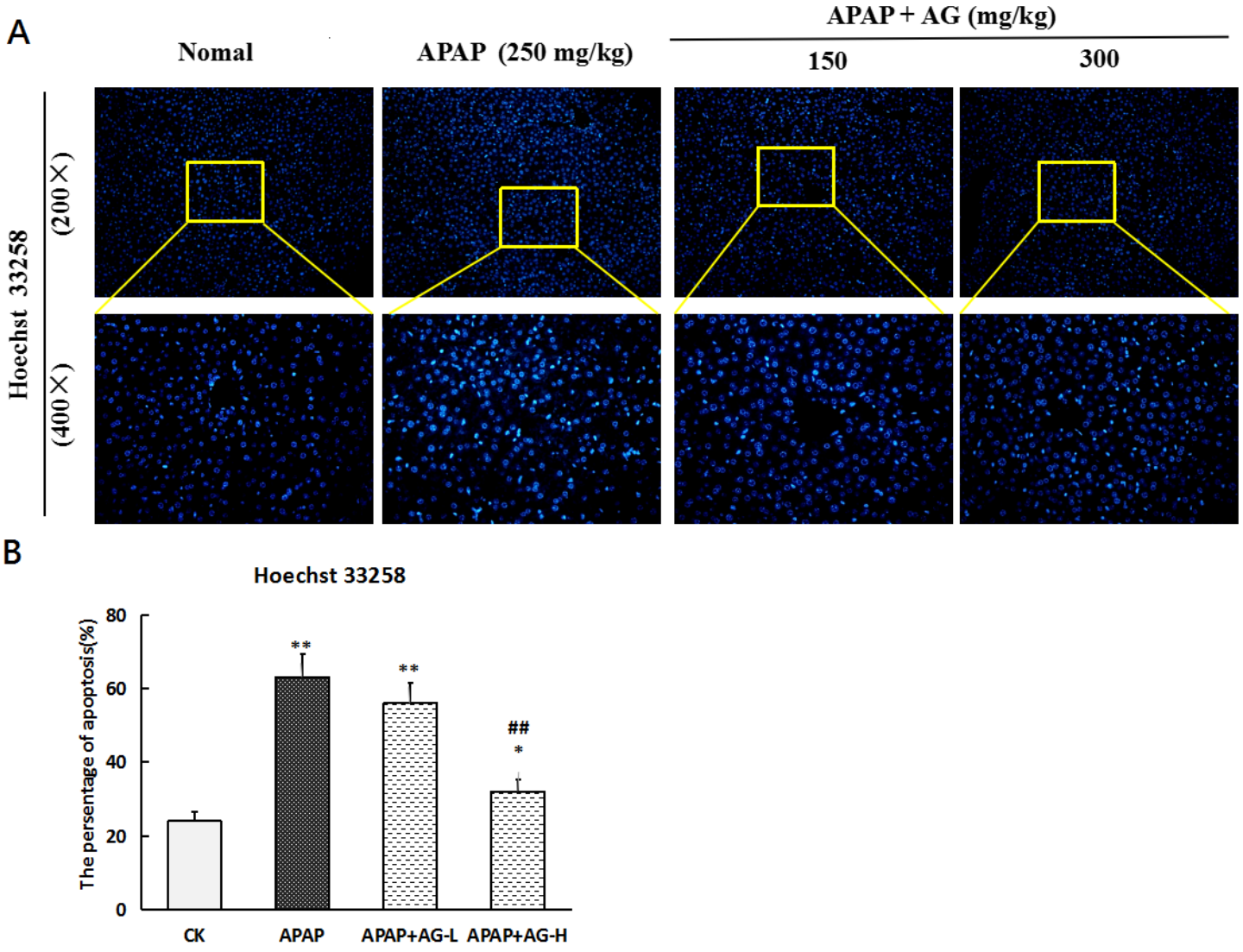

Figure 5

AG pretreatment regulates APAP-induced apoptosis of mouse hepatocytes. **(A)**Liver tissues were stained with Hoechset 33,258 (200 ×, 400 ×) . **(B)** Percentage of Hoechst 33,258 (B) positive cells by image analyzer. (mean ± SD., n = 6. *p < 0.05, **p < 0.01 vs. normal group; #p < 0.05, ##p < 0.01 vs. APAP group).

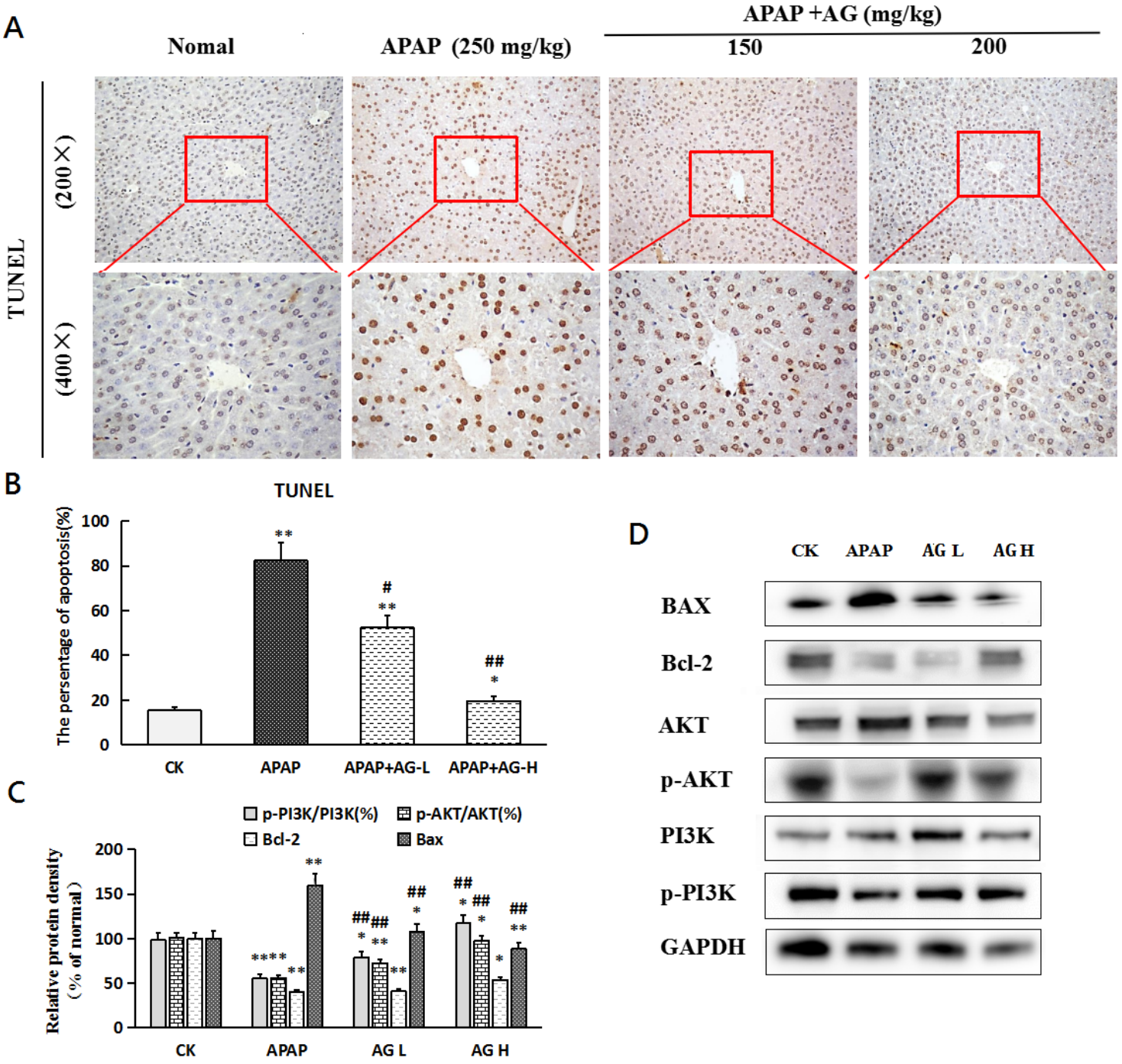

Figure 6

Analysis of AG-regulated apoptosis. (A) Liver tissue was stained with TUNEL (200 ×, 400 ×). (B) Percentage of TUNEL positive cells by image analyzer; Western blot analysis.(C) Quantification of relative protein expression of p-PI3K/PI3K, p-AKT/AKT, Bax and Bcl-2. Values represent mean ± SD,(D)The protein expressions of BAX, Bcl-2, AKT, p-AKT, PI3K, p-PI3K, (mean ± SD., n = 6. *p < 0.05, **p < 0.01 vs. normal group; #p < 0.05, ##p < 0.01 vs. APAP group).

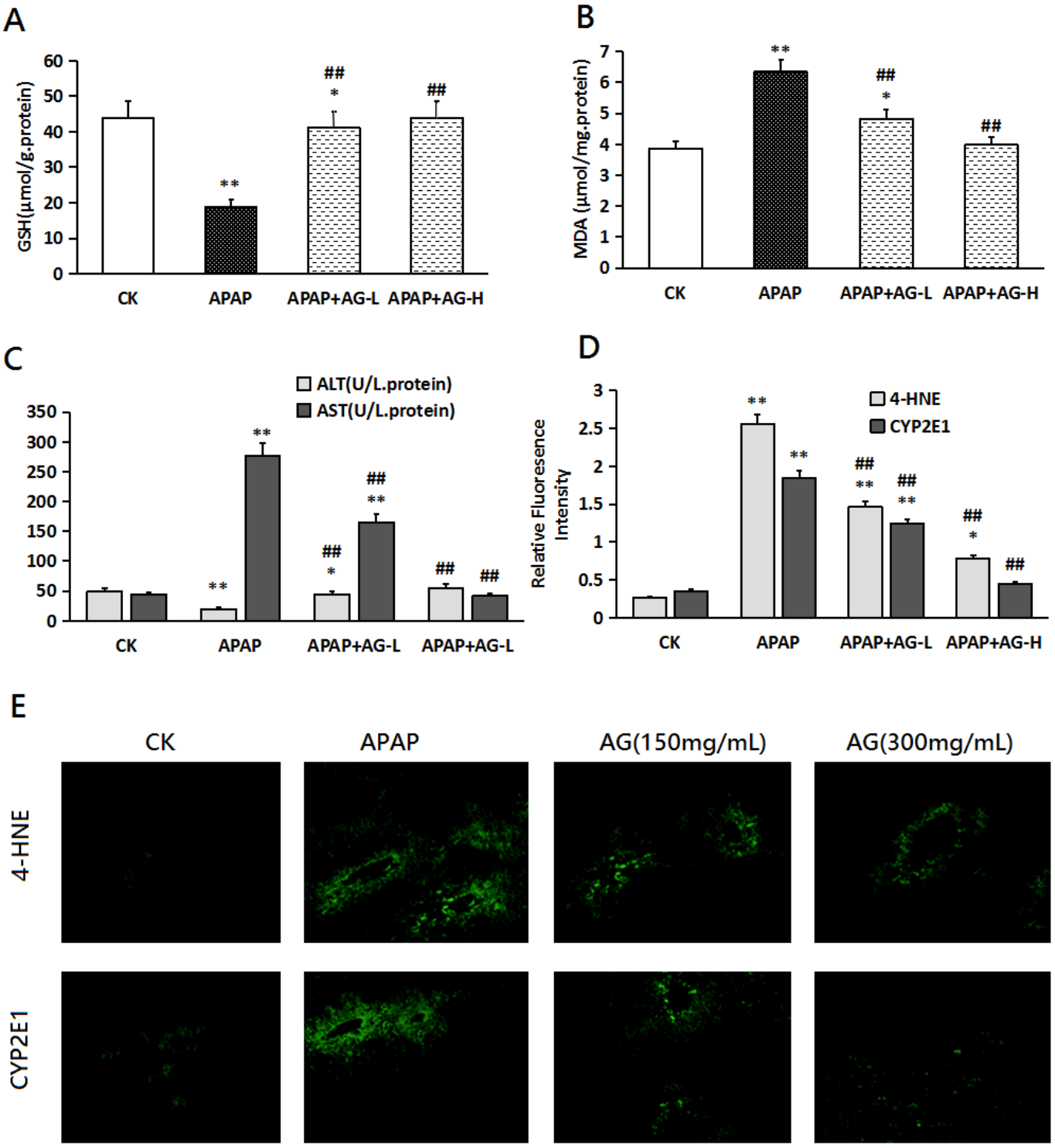

Figure 7

AG protected liver against emergency injury. (A) GSH and (B) MDA level in liver. (C) ALT and AST level in serum.(D) The relative fluorescence intensity of CYP2E1 and 4-HNE. (E) CYP2E and 4-HNE immunofluorescence images. The immunofluorescence methods was used to assess the the expression level of CYP2E1 and 4HNE (Green) in tissue sections isolated from different groups. Representative

immunofluorescence images were taken at 400×. (mean ± SD., n = 6. *p < 0.05, **p < 0.01 vs. normal group; #p < 0.05, ##p < 0.01 vs. APAP group).